

Neutron-scattering spectra of noncubic cerium Kondo compounds

L. C. Lopes

Instituto de Física, Universidade Federal do Rio de Janeiro, 21944 Rio de Janeiro, Brazil

B. Coqblin

Laboratoire de Physique des Solides, Bâtiment 510, Université Paris-Sud, Centre d'Orsay 91405 Orsay, France

(Received 5 May 1988)

Neutron-scattering spectra are computed for noncubic cerium Kondo compounds within the effective resonant-scattering Hamiltonian which describes both Kondo and crystal-field effects, thus extending to noncubic compounds a previous calculation [Phys. Rev. B **33**, 1804 (1986)]. Both the longitudinal and transverse susceptibilities are taken into account, and the results depend on the nature of the ground state considered. The model is finally applied to the experimental neutron-scattering spectra of CeAl₃ and CeCu₂Si₂ compounds.

I. INTRODUCTION

Many neutron-scattering experiments are currently available in anomalous rare-earth compounds.¹⁻⁴ In the case of cerium Kondo compounds, two striking points have been extensively studied in recent years. On one hand, a very broad quasielastic line is observed in neutron-scattering spectra; the deduced quasielastic linewidth starts generally from a finite value at very low temperatures and increases with temperature according to different laws for the temperature dependence.

On the other hand, inelastic lines due to crystal-field excitations have been observed in some cerium compounds. An inelastic peak has been observed in the two cubic compounds CeMg₃ (Ref. 5) at roughly 200 K and CeB₆ (Ref. 6) at 530 K. Neutron-scattering spectra are also available in hexagonal CeAl₃ (Refs. 7 and 8) or tetragonal CeCu₂Si₂ (Refs. 3 and 9): Two extremely weak inelastic lines can be observed at roughly 50 and 100 K in CeAl₃,⁸ while two weak, but clearly visible, inelastic lines are observed at roughly 150 and 300 K in CeCu₂Si₂.⁹

The calculation of the neutron-scattering spectrum¹⁰ within the projection operator method has been performed for the effective resonant scattering Hamiltonian¹¹ in the case of a cubic crystalline field up to second order in the exchange integrals.¹⁰ The dynamical susceptibility and the resulting neutron-scattering quasidelectric linewidth have recently been computed by several authors using self-consistent perturbation theory¹² or the $1/N_f$ expansion technique,¹³ where N_f is the $4f$ level degeneracy. In particular, Hohn and Keller¹² have computed the dynamical susceptibility for the degenerate Anderson Hamiltonian and they have derived a neutron-scattering spectrum with broad quasielastic peaks in the Kondo limit with a cubic crystalline field; however, surprisingly they have found a really much larger quasielastic linewidth than the value obtained by second-order perturbation using the resonant scattering Hamiltonian.¹⁰

The previous calculation¹⁰ has been made only for cubic cerium Kondo compounds, where the $4f^1$

configuration is split into a doublet Γ_7 state and a quartet Γ_8 state. The purpose of this paper is to extend the previous calculation to the case of a noncubic crystal field, splitting the $4f^1$ configuration into three doublets.

II. THE THEORETICAL MODEL

We discuss here the case of a cerium atom with a noncubic crystal field, which splits the $4f^1$ configuration into three doublets corresponding to the quantum numbers $M = \pm\frac{1}{2}, \pm\frac{3}{2}, \pm\frac{5}{2}$. This calculation could be applied directly to the case of hexagonal CeAl₃, but the application to tetragonal CeCu₂Si₂ would be less straightforward since the ground state and the highest excited state are linear combinations of $\pm\frac{3}{2}$ and $\pm\frac{5}{2}$ states, according to neutron-scattering experiments on CeCu₂Si₂.⁹ We will discuss this problem in the Sect. IV.

Thus, here we will compute the neutron-scattering spectrum within the projection-operator technique¹⁴ and we will follow the method previously presented for the cubic case.¹⁰ The effective resonant-scattering Hamiltonian appropriate for the $4f^1$ configuration of cerium is given by¹¹

$$H_{kf} = - \sum_{\substack{k, k' \\ M, M'}} J_{MM'} c_{k'M}^* c_{kM} (c_M^* c_{M'} - \delta_{MM'} \langle n_M \rangle) \quad (1)$$

with the usual notations of Ref. 11: c_M^\dagger is the creation operator for a $4f$ electron localized on cerium, of total angular momentum $j = \frac{5}{2}$ and z component $M = j_z$ for each $4f$ eigenfunction, and c_{kM}^* is the creation operator for a conduction electron with partial wave number k , $j = \frac{5}{2}$, and z component $M = j_z$. The exchange integrals $J_{MM'} (< 0)$ are given, as usual,¹¹ by

$$J_{MM'} = \frac{|V_{kf}|^2}{2} \left[\frac{1}{E_M} + \frac{1}{E_{M'}} \right], \quad (2)$$

where V_{kf} is the k - f mixing potential. In the present case of noncubic cerium compounds, the $4f^1$ configuration is split into three doublets corresponding to

M values equal to $\pm\frac{1}{2}$, $\pm\frac{3}{2}$, and $\pm\frac{5}{2}$, respectively, and there are three energies E_M (< 0) from each doublet to the conduction-band Fermi level. There are, therefore, six different exchange integrals.

Moreover, the susceptibility involved in the calculation of the neutron scattering is no more isotropic, in contrast to the cubic case.¹⁰ The neutron-scattering spectrum is given by $\text{Im}\chi(\omega)\coth(\omega/2T)$, where $\chi(\omega)$ is the total susceptibility equal to

$$\chi(\omega) = \frac{1}{3}\chi_{zz}(\omega) + \frac{2}{3}\chi_{-+}(\omega). \quad (3)$$

Thus, we need to compute here both the longitudinal susceptibility $\chi_{zz}(\omega)$ and the transverse susceptibility $\chi_{-+}(\omega)$. We follow the method presented in Refs. 10 and 14 and we use Eqs. (3)–(14) of Ref. 10 for the calculation of the longitudinal susceptibility; for the calculation of the transverse susceptibility, we change j_z into j_+ and we decompose j_+ as a function of $K_{MM'} = |M\rangle\langle M'|$.

For the calculation of the longitudinal susceptibility, we write the decomposition of j_z as a function of the $K_{MM'}$, where M is now one of the six states $\pm\frac{1}{2}$, $\pm\frac{3}{2}$, $\pm\frac{5}{2}$:

$$\begin{aligned} j_z &= \frac{1}{2}(K_{1/2\ 1/2} - K_{-1/2\ -1/2}) \\ &\quad + \frac{3}{2}(K_{3/2\ 3/2} - K_{-3/2\ -3/2}) \\ &\quad + \frac{5}{2}(K_{5/2\ 5/2} - K_{-5/2\ -5/2}), \\ j_z &= \sum_{M=1}^3 A_M^z. \end{aligned} \quad (4)$$

Similarly, for the calculation of the transverse susceptibility, the decomposition of j_+ can be written as

$$\begin{aligned} j_+ &= \sqrt{5}K_{5/2\ 3/2} + \sqrt{8}K_{3/2\ 1/2} + 3K_{1/2\ -1/2} \\ &\quad + \sqrt{8}K_{-1/2\ -3/2} + \sqrt{5}K_{-3/2\ -5/2}, \end{aligned} \quad (5)$$

$$j_+ = \sum_{M=1}^5 A_M^+.$$

Thus, as previously,¹⁰ we perform partial summations belonging to the same transition energy and with a zero expectation value; the resulting A_μ terms given by Eq. (9) of Ref. 10 are given either by

$$A_M^z = M(K_{MM} - K_{-M\ -M}) \quad (6)$$

for the three A_M^z terms corresponding to $\chi_{zz}(\omega)$ or by

$$A_M^+ = \sqrt{j(j+1) - M(M-1)}K_{MM-1} \quad (7)$$

for the five A_M^+ terms corresponding to $\chi_{-+}(\omega)$.

The calculations follow then the method presented in Ref. 10 and we recall here the main results. The scalar product defined by Eq. (5) of Ref. 10 of two K_{nm} is given, at the lowest zero-order terms, by:

$$(K_{nm} | K_{n'm'}) = \delta_{nn'}\delta_{mm'}T \frac{p_m - p_n}{\omega_{nm}}, \quad (8)$$

where $\omega_{nm} = E_n - E_m$ and p_m is the thermal occupation of the state labeled by the index m .

The matrix element $M_{stnm}(Z)$ of the memory function defined by Eq. (23) of Ref. 10, i.e.,

$$M_{stnm}(Z) = \left[\mathcal{L}_{kf}K_{st} \left| \frac{1}{\mathcal{L}_0 - Z} \mathcal{L}_{kf}K_{nm} \right|_0 \right] \quad (9)$$

is given by^{10,15}

$$M_{stnm}(Z) = \frac{T}{Z} \left[\delta_{tm}\delta_{sn} \sum_M [|J_{Mm}|^2 \Delta F_{nM}(Z) + |J_{nM}|^2 \Delta F_{Mm}(Z)] - \delta_{mn}\delta_{st} |J_{ns}|^2 [\Delta F_{ns}(Z) + \Delta F_{sn}(Z)] \right]. \quad (10)$$

In formulas (9) and 10, \mathcal{L}_0 and \mathcal{L}_{kf} are the Liouville operators corresponding, respectively, to the one-body Hamiltonian H_0 describing the $4f^1$ configuration and the conduction electrons, and the Hamiltonian H_{kf} given by (1) and

$$\Delta F_{nm}(Z) = F_{nm}(Z) - F_{nm}(0) \quad (11)$$

with

$$F_{nm}(Z) = \sum_{k,q} \frac{f_k(1-f_{k+q})p_m - f_{k+q}(1-f_k)p_n}{\omega_{nm} + \varepsilon_{k+q} - \varepsilon_k - Z}. \quad (12)$$

We follow the method presented in Ref. 10 from Eq. (30) to Eq. (35) and in particular the analytical expressions of $F_{nm}(Z)$ derived in Ref. 14. thus, we use in the following the notations

$$P_{ii}^z = (A_i^z | A_i^z), \quad (13)$$

$$M_{ii}^z(\omega) = \left[\mathcal{L}_{kf}A_i^z \left| \frac{1}{\mathcal{L}_0 - \omega} \mathcal{L}_{kf}A_i^z \right| \right] \quad (14)$$

for the values corresponding to the longitudinal susceptibility; the same formulas hold for the values corresponding to the transverse susceptibility with the only change of the superscript z to $+$.

Let us discuss the shape of the neutron-scattering spectrum given by $\text{Im}\chi(\omega)\coth(\omega/2T)$. The longitudinal part $\text{Im}\chi_{zz}(\omega)$ of the spectrum is the sum of three Longitudinal functions, i.e.,

$$\text{Im}\chi_{zz}(\omega) = \frac{\omega}{T} \sum_{i=1}^3 \frac{\text{Im}M_{ii}^z(\omega)}{\omega^2 + [(P_{ii}^z)^{-1}\text{Im}M_{ii}^z(\omega)]^2}. \quad (15)$$

The three Lorentzian functions are centered at $\omega=0$ and contribute only to the quasielastic line, each of them

having a width equal to $(P_{ii}^z)^{-1} \text{Im}M_{ii}^z(\omega)$. Each Lorentzian function corresponds to elastic transitions within each doublet and there is no inelastic transition with the longitudinal part.

On the other hand, the transverse part $\text{Im}\chi_{-+}(\omega)$ of the spectrum is the sum of five Lorentzian functions, i.e.,

$$\text{Im}\chi_{-+}^{(\omega)} = \frac{\omega}{T} \sum_{i=1}^5 \frac{\text{Im}M_{ii}^+(\omega)}{(\omega - \omega_i)^2 + [(P_{ii}^+)^{-1} \text{Im}M_{ii}^+(\omega)]^2}. \quad (16)$$

Among the five Lorentzian functions, there is one elastic line labeled $i=3$ corresponding to the transition within the doublet $\pm\frac{1}{2}$. The four other lines are inelastic ones and are centered at energies $\omega_1 = E_{5/2} - E_{3/2}$, $\omega_2 = E_{3/2} - E_{1/2}$, $\omega_4 = -\omega_2$, and $\omega_5 = -\omega_1$. It results that, at very low temperatures ($T \ll |\omega_1|$ and $|\omega_2|$), there is an elastic contribution to the transverse susceptibility only if the ground state is the state $\pm\frac{1}{2}$.

Since we are interested here only in positive ω values, the neutron-scattering spectrum has an elastic line and two inelastic lines centered at $\Delta_1 = |\omega_1| = |\omega_5|$ and $\Delta_2 = |\omega_2| = |\omega_4|$, except in the accidental case where Δ_1 and Δ_2 are equal to or close to each other. The elastic line comes, therefore, from the transition from $+\frac{1}{2}$ to $-\frac{1}{2}$ for χ_{-+} and from the three transitions of χ_{zz} , while the two inelastic lines correspond, respectively, to either the transition from $+\frac{5}{2}$ to $+\frac{3}{2}$ or from $-\frac{3}{2}$ to $-\frac{5}{2}$ (according to whether ω_1 or ω_5 is positive) and to either the transition from $+\frac{3}{2}$ to $+\frac{1}{2}$ or from $-\frac{1}{2}$ to $-\frac{3}{2}$ (according to whether ω_2 or ω_4 is positive).

Before presenting in the next section the numerical results for the neutron-scattering spectra, let us examine here the low-temperature and the high-temperature limits for the quasi elastic and inelastic linewidths.

At low temperatures, $T \ll \Delta_1$ and Δ_2 , the quasielastic line is obtained by the four Lorentzian functions corresponding to the three functions of χ_{zz} and to the $i=3$ function of χ_{-+} . At low temperatures, only the ground-state doublet is occupied and the linewidths of the four Lorentzian functions, which are, respectively, equal to $(P_{ii}^z)^{-1} \text{Im}M_{ii}^z(\omega)$ (with $i=1,2,3$) or to $(P_{33}^+)^{-1} \text{Im}M_{33}^+(\omega)$, become equal to each other. Thus, the quasielastic linewidth, which is equal to their common value, is given by

$$\delta_{\text{qe}} = 4\pi |n(E_F) J_{11}|^2 T, \quad (17)$$

where $n(E_F)$ and J_{11} are, respectively, the density of states of the conduction band at the Fermi energy for one spin direction and the exchange integral for the ground-state doublet, independent of their M values. However, the intensity of the maximum value at $\omega=0$ of the quasielastic line depends at low temperatures on the nature of the ground state. According to (15) and (16), the $\omega=0$ intensity I of the neutron-scattering quasielastic line is given by

$$I = \lim_{\omega \rightarrow 0} \text{Im}\chi(\omega) \coth(\omega/2T) \\ = \frac{2}{3(\gamma_{\text{qe}})^2} \text{Im}[M_{ii}^z(0) + 2M_{33}^+(0)\delta_{i3}]. \quad (18)$$

The last term of (18) is nonzero only if the ground state is the $\pm\frac{1}{2}$ doublet.

Thus, the intensity I of the quasielastic line at $\omega=0$ is equal to

$$I = \frac{D_M}{6\gamma_{\text{qe}}}, \quad (19)$$

where γ_{qe} is given by the low-temperature expression (17) and the coefficient $D_M=37$ for the $\pm\frac{1}{2}$ ground state. $D_M=9$ for the $\pm\frac{3}{2}$ ground state, and $D_M=25$ for the $\pm\frac{5}{2}$ ground state. We see that, for the $\pm\frac{1}{2}$ ground state, there is a contribution of 36 from the transverse susceptibility and of 1 from the longitudinal one, while D_M originates only from the longitudinal one for the $\pm\frac{3}{2}$ and $\pm\frac{5}{2}$ ground states.

In conclusion, at low temperatures, the half-width of the quasielastic line is, therefore, always given by (17), but the intensity of the quasielastic peak must be much larger for the $\pm\frac{1}{2}$ ground state than for the $\pm\frac{3}{2}$ and $\pm\frac{5}{2}$ ground states, if all the other parameters remain unchanged.

Let us give now the low-temperature behavior for the half linewidth γ_{in} of the inelastic lines centered at Δ_1 or Δ_2 and corresponding to $\pm\frac{5}{2} \leftrightarrow \pm\frac{3}{2}$ or $\pm\frac{3}{2} \leftrightarrow \pm\frac{1}{2}$ transitions; there is no transition corresponding to $\pm\frac{5}{2} \leftrightarrow \pm\frac{1}{2}$ in this model. The low-temperature behavior of γ_{in} depends on the scheme of levels split by the crystalline field. In our present case of three doublets split by the crystalline field, there are three possible behaviors for the inelastic lines and their widths:

(i) The first case corresponds to an inelastic line at a position energy Δ_{21} describing the transition between the state n on the first excited doublet (labeled 2) to the state m on the ground-state doublet (labeled 1). The half-width γ_{in} of this inelastic line, which is given by $(P_{ii}^+)^{-1} \text{Im}M_{ii}^+(\omega)$ for the i th considered transition with $\omega = \Delta_{21}$, is given, at low temperatures ($T \ll \Delta_{21}$), by

$$\gamma_{\text{in}} = 2\pi n (E_F)^2 [|J_{21}|^2 \Delta_{21} + (|J_{11}|^2 + |J_{22}|^2) T], \quad (20)$$

where we have considered only the zero- and first-order terms in T and where the indices of J_{ij} refer obviously to the two levels 1 and 2.

We see that γ_{in} has a finite value at $T=0$, exactly as in the previous cubic case,¹⁰ and that γ_{in} is linear in T at low temperatures.

(ii) The second case corresponds to an inelastic line at a positive energy Δ_{31} describing the transition between the state n on the second- or highest-excited doublet (labeled 3) to the state m on the ground state 1. The half-width γ_{in} of this inelastic line is given, at low temperatures ($T \ll \Delta_{21}$), by

$$\gamma_{\text{in}} = 2\pi n (E_F)^2 [|J_{31}|^2 \Delta_{31} + |J_{32}|^2 \Delta_{32} \\ + (|J_{11}|^2 + |J_{33}|^2) T]. \quad (21)$$

The $T=0$ value of the half-width given by (21) is larger here than in preceding case and differs from the result in the cubic case.¹⁰ We can notice that the slope of the linewidth versus T is the same for the elastic line and the

different cases for the inelastic line, if we take all the $J_{MM'}$ equal to one another.

(iii) The third case corresponds to a transition between the state n on the second-excited doublet 3 and the state m on the first-excited doublet 2. Since the two levels are empty at low temperatures, there is no inelastic transition corresponding to this transition at $T=0$ and very low temperatures ($T \ll \Delta_{21}$). Clearly, this case is different from the two preceding ones, since the inelastic line appears slowly with increasing temperature and its intensity is, therefore, firstly increasing, while the intensity of the inelastic lines in the two preceding cases is always decreasing with temperature.

Let us examine the high-temperature ($T \gg \Delta_{31}$ and Δ_{21}) behavior of the quasielastic and inelastic linewidths. At high temperatures, the linewidths of the four Lorentzian functions giving rise to the quasielastic line are also equal to each other and the resulting half-width γ_{qe} of the quasielastic line is given, for $T \gg \Delta_{31}$, by

$$\gamma_{qe} = 4\pi n (E_F)^2 (|J_{11}|^2 + |J_{12}|^2 + |J_{13}|^2) T. \quad (22)$$

Similarly, the half-width γ_{in} of an inelastic line corresponding to a transition from a level n to a level m is given, at high temperatures, by

$$\gamma_{in} = 2\pi n (E_F)^2 (|J_{n1}|^2 + |J_{n2}|^2 + |J_{n3}|^2 + |J_{m1}|^2 + |J_{m2}|^2 + |J_{m3}|^2). \quad (23)$$

We see immediately that, at high temperatures, the half-widths of all the lines become equal to each other and are given by

$$\gamma = 12\pi |n(E_F)J|^2 T \quad (24)$$

if all the $J_{MM'}$ values are taken equal to J .

Thus, we recover the previous result¹⁰ that, if we take all the $J_{MM'}$ values equal to J , the ratio of the high- and low-temperature slopes of the quasielastic linewidth versus temperature is 3, i.e., exactly the ratio of the effective degeneracies of the occupied $4f$ levels. Moreover, in the present case of three doublets, we find also the same result for the ratio of the high- and low-temperature slopes of the inelastic linewidths versus temperature.

III. RESULTS FOR THE NEUTRON-SCATTERING SPECTRUM

Some numerical results for the neutron-scattering spectrum for a noncubic cerium Kondo compound are presented in Figs. 1–4. We use for these figures a reasonable set of common parameters: the three doublets lie, respectively, at -450 K, -400 K, and -350 K below the Fermi energy; the hybridization parameter is $V_{kf} = 700$ K, so that the exchange integral J_{11} for the ground state is always equal to $J_{11} = -0.094$ eV; moreover, the density of states of the conduction band is taken equal to $n(E_F) = 0.93$ states/eV atom for one spin direction and the cutoff energy D is taken equal to $D = 850$ K, as previously.^{10,11} The two variable parameters here are the nature of the different doublets and the temperature.

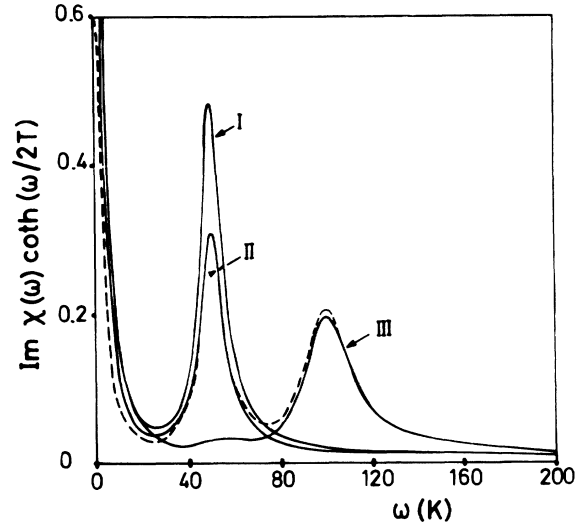


FIG. 1. Plot of $\text{Im}\chi(\omega)\coth(\omega/2T)$ vs ω (in K) at 20 K for four different crystalline field level schemes: case I corresponds to the sequence $(\pm\frac{1}{2}, \pm\frac{3}{2}, \pm\frac{5}{2})$; case II to $(\pm\frac{5}{2}, \pm\frac{3}{2}, \pm\frac{1}{2})$; case III to $(\pm\frac{1}{2}, \pm\frac{5}{2}, \pm\frac{3}{2})$; and case IV (plotted as a dashed line) to $(\pm\frac{3}{2}, \pm\frac{5}{2}, \pm\frac{1}{2})$. The following parameters are used: the three doublets lie at, respectively, -450 K, -400 K, and -350 K below the Fermi energy, $V_{kf} = 700$ K and $n(E_F) = 0.93$ states/eV atom. The values of $\text{Im}\chi(\omega)\coth(\omega/2T)$ at $\omega=0$ are equal to 2.32 in cases I and III, 1.57 in case II, and 0.6 in case IV.

Figure 1 shows firstly the neutron-scattering spectrum $\text{Im}\chi(\omega)\coth(\omega/2T)$ versus ω at 20 K with the preceding parameters. The plots correspond to different crystalline field level schemes: either the sequence $\pm\frac{1}{2}, \pm\frac{3}{2}, \pm\frac{5}{2}$ (case I) (the levels are labeled according to increasing energy and $\pm\frac{1}{2}$ is here the ground state), which gives only a peak

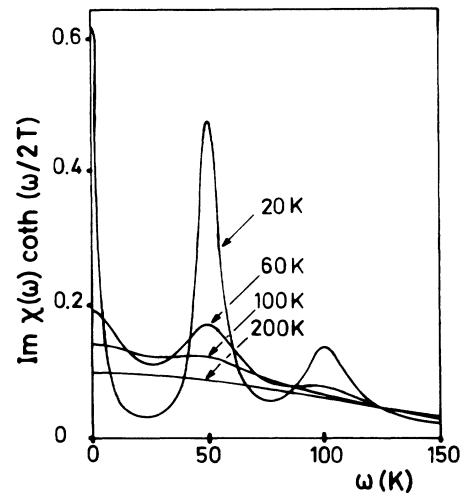


FIG. 2. Plot of $\text{Im}\chi(\omega)\coth(\omega/2T)$ vs ω (in K) at different temperatures, for a $\pm\frac{3}{2}$ ground state and the $(\pm\frac{3}{2}, \pm\frac{1}{2}, \pm\frac{5}{2})$ crystalline field level sequence. The parameters used here are the same as those of Fig. 1.

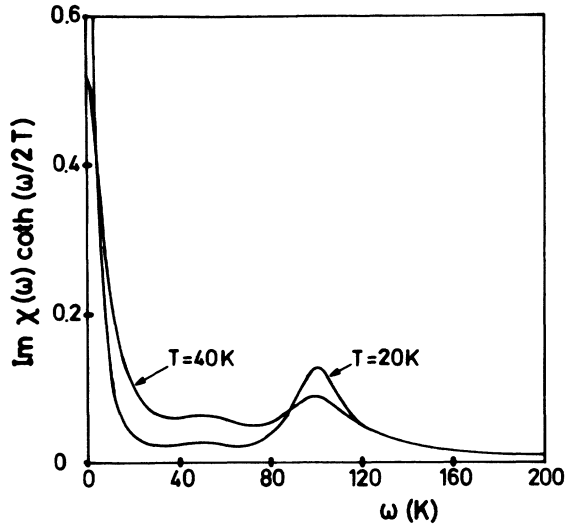


FIG. 3. Plot of $\text{Im}\chi(\omega)\coth(\omega/2T)$ vs ω (in K) at 20 K and 40 K for a $\pm\frac{5}{2}$ ground state and the $(\pm\frac{5}{2}, \pm\frac{1}{2}\pm\frac{3}{2})$ crystalline field level sequence. The parameters used here are the same as those of Fig. 1. The value of $\text{Im}\chi(\omega)\coth(\omega/2T)$ at $\omega=0$ is equal to 1.6 at 20 K.

at 50 K for the transition $\pm\frac{3}{2}\rightarrow\pm\frac{1}{2}$; or the sequence $\pm\frac{5}{2}, \pm\frac{3}{2}, \pm\frac{1}{2}$ (case II) which gives also a peak at 50 K for the transition $\pm\frac{5}{2}\rightarrow\pm\frac{3}{2}$; or the sequence $\pm\frac{1}{2}, \pm\frac{5}{2}, \pm\frac{3}{2}$ (case III) which gives now only a peak at 100 K for the transition $\pm\frac{3}{2}\rightarrow\pm\frac{1}{2}$; or finally the sequence $\pm\frac{3}{2}, \pm\frac{5}{2}, \pm\frac{1}{2}$ (case IV) (plotted as a dashed line) which gives two peaks

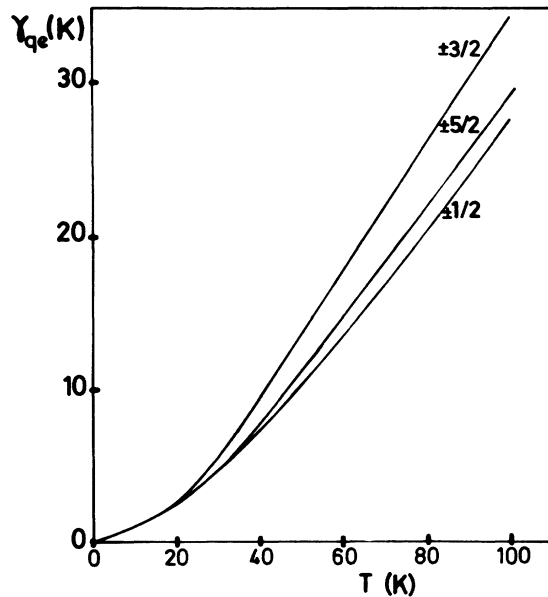


FIG. 4. Plot of the half-widths γ_{qe} (in K) for a $\pm\frac{1}{2}$ or a $\pm\frac{3}{2}$ or a $\pm\frac{5}{2}$ ground state. The parameters used here are the same as those of Fig. 1.

at 50 K and 100 K corresponding to the two transitions $\pm\frac{5}{2}\rightarrow\pm\frac{3}{2}$ and $\pm\frac{1}{2}\rightarrow\pm\frac{3}{2}$. The occurrence of these different peaks corresponds obviously to the low-temperature behavior described in the preceding section. Moreover, two points must be emphasized: First, the peak width observed at 100 K is much larger than that at 50 K according to formulas (20) and (21); second, the heights of the $\omega=0$ peaks are equal, in Fig. 1 at 20 K, to 2.32 (cases I and III), 1.57 (case II), and 0.6 (case IV with dashed line), which agrees with expression (19) with a coefficient D_M , respectively equal to 37, 25, and 9 according to the considered ground state.

Figure 2 shows the neutron-scattering spectrum versus ω at different temperatures with the sequence $\pm\frac{3}{2}, \pm\frac{1}{2}, \pm\frac{5}{2}$ for the crystalline field level scheme; at low temperatures, there are two inelastic peaks at 50 K and 100 K corresponding to the $\pm\frac{1}{2}\rightarrow\pm\frac{3}{2}$ and $\pm\frac{5}{2}\rightarrow\pm\frac{3}{2}$ transitions. We see that the intensities of the peaks decrease with increasing temperature and that the spectrum is flat at 200 K. This situation is similar to that previously observed in the cubic case.¹⁰

Figure 3 shows the neutron-scattering spectrum versus ω at 20 and 40 K with the sequence $\pm\frac{5}{2}, \pm\frac{1}{2}, \pm\frac{3}{2}$ for the crystalline field level scheme; at low temperatures, there is only one peak at 100 K corresponding to the transition from the highest excited level $\pm\frac{3}{2}$ to the ground state $\pm\frac{5}{2}$; the intensity of this peak decreases with increasing temperature. On the contrary, there is no inelastic peak at the $\omega=50$ K energy at very low temperatures, but the intensity at $\omega=50$ K increases with increasing temperature and a very weak peak is visible at $T=40$ K.

Finally, Fig. 4 gives the plots versus temperature of the quasielastic half-widths γ_{qe} for the same parameters and for either a $\pm\frac{1}{2}$, or a $\pm\frac{3}{2}$, or a $\pm\frac{5}{2}$ ground state. We have not plotted in Fig. 4 the different γ_{qe} values when we change the two excited states without changing the ground state, because the observed differences on γ_{qe} are almost negligible. Moreover, as shown in Fig. 4, the temperature dependence of γ_{qe} is not greatly dependent on the nature of the ground state. But, as in the cubic case,¹⁰ the half-width γ_{qe} of the quasielastic line starts from zero at $T=0$, presents a positive curvature at low temperatures, and behaves linearly with temperature at high temperatures.

IV. COMPARISON WITH EXPERIMENT AND CONCLUDING REMARKS

Thus, the neutron-scattering spectrum for noncubic cerium Kondo compounds presents one or two inelastic peaks, the second case occurring at low temperatures only if the ground state is the $\pm\frac{3}{2}$ doublet.

The typical neutron-scattering spectrum shown in Fig. 2 can account qualitatively for the experimental neutron spectra of hexagonal CeAl_3 and tetragonal CeCu_2Si_2 , where two weak inelastic lines have been observed. In fact, the theoretical parameters used in Figs. 1–4 have been chosen to fit the case of CeAl_3 , where the ground state is known to be the $\pm\frac{3}{2}$ doublet, and where also the two experimental inelastic lines are located at roughly 50

and 100 K, and finally in order to take the theoretical and experimental values of γ_{qe} equal to each other at 100 K.

The case of CeCu_2Si_2 is more delicate, since the ground-state level 1 and the second-excited level 3 are linear combinations of $\pm\frac{3}{2}$ and $\pm\frac{5}{2}$ states, while the first-excited level 2 is a pure $\pm\frac{1}{2}$ state, according to magnetic neutron-scattering experiments of Horn *et al.*⁹ Thus, there are additional elastic and inelastic transitions occurring from both the longitudinal and transverse susceptibilities, with respect to the present analysis. However, there appear two inelastic peaks at low temperatures at roughly 150 and 300 K,⁹ corresponding to the transitions $\pm\frac{1}{2} \leftrightarrow \pm\frac{3}{2}$ and $\frac{5}{2} \leftrightarrow \pm\frac{3}{2}$ between, respectively, the states $2 \leftrightarrow 1$ and $3 \leftrightarrow 1$. A more complete analysis of the case of CeCu_2Si_2 could be straightforwardly performed in view of more detailed experimental neutron-scattering results.

But, the shape of the γ_{qe} versus T curve is not the same, since the theoretical one is linear above 40 K as shown in Fig. 4 and the experimental one clearly has a negative curvature. Moreover, the very low-temperature experimental value of γ_{qe} has a finite value; but, the

present model is no more valid at very low temperatures below the Kondo temperature T_k in cerium Kondo compounds, and a finite residual linewidth is obtained within the spin-fluctuation model¹⁶ which is certainly more appropriate in such systems below T_k . Indeed, the remarks on the validity of the model previously presented for the cubic case¹⁰ hold also in this case.

Despite its deficiencies, our model can, therefore, account for the neutron-scattering spectra in noncubic cerium Kondo compounds. Further experiments, such as, for example, the study of the occurrence of one or two peaks as a function of the considered ground state and of the temperature dependence of the linewidth in noncubic cerium Kondo compounds, would be interesting to check the present theoretical model.

ACKNOWLEDGMENTS

The Laboratoire de Physique des Solides is "Laboratoire associé au C.N.R.S." One of us (L.C.L.) thanks the C. N. Pq (Brazilian Council for Scientific and Technological Development) for a research fellowship.

- ¹M. Loewenhaupt and E. Holland-Moritz, *J. Appl. Phys.* **50**, 7456 (1979); *J. Magn. Magn. Mater.* **14**, 227 (1979).
²M. Loewenhaupt, B. D. Rainford, and F. Steglich, *Phys. Rev. Lett.* **42**, 1709 (1979).
³S. Horn, F. Steglich, M. Loewenhaupt, and E. Holland-Moritz, *Physica* **107B**, 103 (1981).
⁴E. Holland-Moritz, D. Wohlleben, and M. Loewenhaupt, *Phys. Rev. B* **25**, 7482 (1982).
⁵J. Pierre, A. P. Murani, and R. M. Galera, *J. Phys. F* **11**, 679 (1981).
⁶E. Zirngiebl, B. Hillebrands, S. Blumerröder, G. Güntherodt, M. Loewenhaupt, J. M. Carpenter, K. Winzer, and Z. Fisk, *Phys. Rev. B* **30**, 4052 (1984).
⁷A. P. Murani, K. Knorr, K. H. J. Buschow, A. Benoit, and J. Flouquet, *Solid State Commun.* **36**, 523 (1980).
⁸P. Alekseev, I. P. Sadikov, I. A. Markova, E. M. Savitskii, V. F. Terekhova, and O. D. Chistyakov, *Fiz. Tverd. Tela (Leningrad)* **18**, 2509 (1976) [*Sov. Phys.-Solid State* **18**, 1466

(1976)].

- ⁹S. Horn, E. Holland-Moritz, M. Loewenhaupt, F. Steglich, H. Scheuer, A. Benoit, and J. Flouquet, *Phys. Rev. B* **23**, 3171 (1981).
¹⁰L. C. Lopes and B. Coqblin, *Phys. Rev. B* **33**, 1804 (1986).
¹¹B. Coqblin and J. R. Schrieffer, *Phys. Rev.* **185**, 847 (1969); B. Cornut and B. Coqblin, *Phys. Rev. B* **5**, 4541 (1972).
¹²T. Höhn and J. Keller, *J. Magn. Magn. Mater.* **63-64**, 219 (1987), and references therein.
¹³O. Gunnarsson and K. Schönhammer, *J. Magn. Magn. Mater.* **52**, 227 (1985).
¹⁴K. W. Becker, P. Fulde, and J. Keller, *Z. Phys. B* **28**, 9 (1977).
¹⁵There is a misprint in the Eq. (25) of Ref. 10, where $\delta_{mn}\delta_{st}$ is forgotten in front of the second term. Formula (10) of this paper is, therefore, the correct one.
¹⁶L. C. Lopes, Y. Lassailly, R. Jullien, and B. Coqblin, *J. Magn. Magn. Mater.* **31-34**, 251 (1983).